12th International Symposium on Turbulence and Shear Flow Phenomena (TSFP12)
Osaka, Japan (Online), July 19-22, 2022

DIRECT NUMERICAL SIMULATION OF ADVERSE PRESSURE GRADIENT TURBULENT BOUNDARY LAYER UP TO $Re_\theta \simeq 8000$

Hussein Rkein
Univ. Lille, CNRS, ONERA, Arts et Metiers Institute of Technology, Centrale Lille,
UMR 9014 -LMFL- F-59000, Lille, France
hussein.rkein@univ-lille.fr

Jean-Philippe LAVAL
Univ. Lille, CNRS, ONERA, Arts et Metiers Institute of Technology, Centrale Lille
UMR 9014 -LMFL- F-59000, Lille, France
jean-philippe.laval@univ-lille.fr

ABSTRACT

A direct numerical simulation of a moderate adverse pressure gradient turbulent boundary layer flow on a flat plate was performed on a fairly long domain with a Reynolds number from $Re_\theta \sim 2000$ to $Re_\theta \sim 8000$. The mean flow and Reynolds stress statistics are analysed. The mean streamwise velocity profile does not exhibit a clear log region even at the highest Reynolds number. The Reynolds stresses exhibit a well defined peak in the outer region which moves away from the wall before to stabilise near 0.45 boundary layer thickness. These outer peaks are the consequences of an excess of production over dissipation. The large scales structures analysed by means of two point correlations of streamwise fluctuating velocity are shown to be strongly modified by the adverse pressure gradient.

Introduction

The accurate prediction of turbulent boundary layer (TBL) remains a significant challenge in many practical problems including engineering design of vehicles, internal aerodynamics or turbomachinery. In order to better understand the physics of such flows, it was natural to concentrate first on flat plate zero pressure gradient (ZPG) TBL. However, ZPG conditions are nearly never encountered in real-life applications as the majority of flow problems encounter the effect of complex pressure gradient on flat or curved walls. The applicability of the knowledge from ZPG TBLs to decelerating boundary layers is still rather limited. Despite many simulations and experiments on adverse pressure gradient (APG) TBLs, there is still no consensus and clear understanding of the main effects of a streamwise adverse pressure gradient, its magnitude and its upstream history on turbulence statistics and large scale coherent structures. Despite many proposals, no universal velocity and length scale are able to successfully re-scale the turbulence statistics for a wide range of flow parameters. In order to study the effect of these APG flow parameters, a large variety of experimental and numerical data are needed to cover a wide range of pressure gradient and Reynolds numbers. Most of detailed databases have been obtained for adverse pressure gradient flows in equilibrium (see Kitsios *et al.* (2017)) either for weak pressure gradient or very strong pressure gradient to focus on the condition before or at the edge of separation. Moreover, only few DNS are available at Reynolds numbers sufficient to decouple the near wall from the outer region of the boundary layer (Lee (2017)). A recent wall resolved LES of APG TBL at Reynolds number up to $Re_\theta \simeq 8700$ with mild adverse pressure gradient has been performed by Pozuelo *et al.* (2022). The effect of a strong adverse pressure gradient has been studied using a DNS of converging diverging channel flow at two Reynolds numbers by Marquillie *et al.* (2008) and Marquillie *et al.* (2011). It has been shown from these studies that a strong peak of production in the adverse pressure gradient region was due to the strengthening of the near-wall streaks instability. However, the Reynolds number was too low to uncouple this near wall effect to the consequence of the APG in the outer region. The aim of the present work is to fill this gap by analysing a new direct numerical simulation (DNS) of APG TBL at moderate and not constant pressure gradient. The present work will focus on velocity scaling as well as streamwise large scale structures and their contribution to Reynolds stresses.

Numerical simulation

A DNS of APG turbulent boundary layer on a flat plate was performed on a fairly large domain with a Reynolds number up to $Re_\theta \sim 8000$. The DNS was simulated using an inlet condition for velocity from a precursor DNS of ZPG TBL at $Re_\theta \sim 2200$ (see Solak & Laval (2018)). As the original DNS was on a smaller domain, the inlet velocity fields have been extrapolated in the normal direction and periodized by a factor of 4 in the spanwise direction. However, to avoid the exact repetition in the results because of duplication of inlet planes, a spatial-temporal noise of small amplitude was added to the inlet velocity components similar to the numerical forcing used by Schlatter *et al.* (2012). The APG is imposed by prescribing the wall normal velocity estimated from a potential flow solution like in Kitsios *et al.* (2017). Neumann Boundary conditions are used for the streamwise velocity by imposing a zero spanwise vorticity. A fringe region has been applied on the last 3% of the computational domain in order to force the laminarity of the outgoing flow. The pressure gradient was chosen to be comparable with an APG TBL experiment from

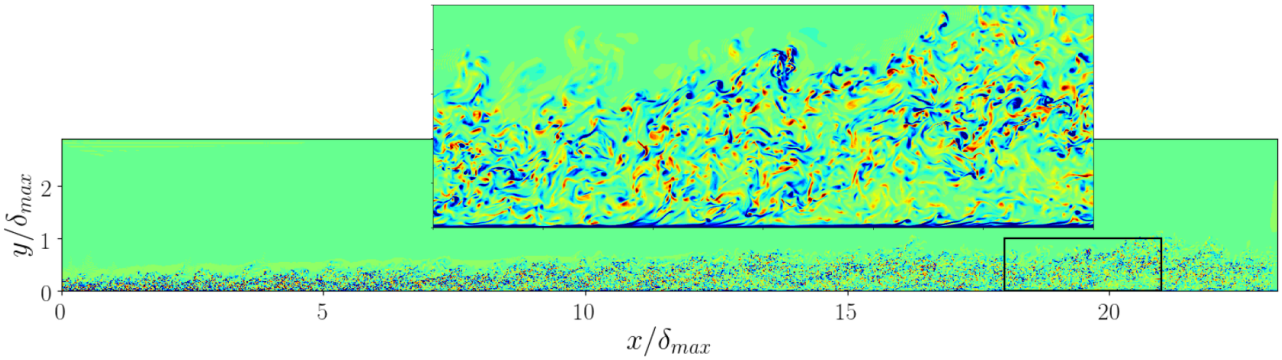

Figure 1. Snapshot of the spanwise vorticity in a streamwise wall-normal plane on the full simulation domain. δ_{max} is the maximum boundary layer thickness at the end of the simulation domain (before the fringe region).

Cuvier *et al.* (2017) on a long ramp in the LMFL wind tunnel at Reynolds number up to $Re_\theta \sim 23000$. It was not possible to reproduce the exact same pressure gradient but the aim is rather to study the Reynolds number effect on a case with comparable APG magnitude.

The DNS has been simulated using the open-source code Incompact3D developed by Laizet & Lamballais (2009). Sixth-order compact finite difference schemes are used for the spatial discretization and third-order Adams-Bashforth scheme for the time advancement using a time step $\Delta t^+ = 0.0125$ based on friction velocity at the outlet. The main parameters of the simulation are given in Table 1. The simulation is well resolved on the full boundary layer thickness (the normal grid resolution at the top of the TBL Δy^+_δ is of the order of 4.7). This allows us to perform detailed and accurate statistics of both large scales and small dissipative scales. A large database of 100TB was recorded with the results on 70 characteristic times $T = \delta_{max}/U_\infty$ after the transient. It is composed of 211 three-dimensional velocity and pressure fields as well as a time evolution (every 1.37 wall unit time) of a 3D restricted domain in the downstream region of the flow ($6818 < Re_\theta < 7582$) and three normal-spanwise planes. A snapshot of the spanwise vorticity in the full simulation domain is shown in Figure 1.

Table 1. Parameters of the APG TBL normalised by the quantities (δ, u_τ) at the outlet. N_x, N_y and N_z are the number of grid points in the streamwise, normal and spanwise direction, L_x, L_y and L_z are the dimensions of the domain and Δx^+, Δy^+, Δz^+ the grid resolution in wall unit (Δy^+_δ being the normal grid size at the top of the boundary layer δ).

Re_θ	$2200-8000$
Re_τ	$750-1400$
N_x, N_y, N_z	6401, 1025, 1280
L_x, L_y, L_z	23.3δ, 2.9δ, 2.33δ
Δx^+, Δy^+_{min}, Δy^+_δ, Δz^+	5.1, 1.0, 4.7, 2.4

Statistical results

The mean streamwise velocity profiles of APG TBL are plotted in Fig. 2 at several streamwise positions and compared with the profiles of ZPG TBL at comparable Reynolds numbers. As already observed the APG leads to a reduction of the log region and an extension of the wake region as compared to the ZPG case at the same Reynolds (either Re_θ or Re_τ). A detailed analysis of the log-law scaling using a diagnostic plot indicates that the profiles exhibit no clear plateau but rather a maximum that moves toward the wall for the lowest Reynolds numbers ($Re_\theta < 3000$) and then moves away from the wall like the square root of Re_θ when moving downstream. This peak does not seem to flatten for any Reynolds numbers indicating that no log region can be identified even at ($Re_\theta > 7000$).

As already noticed for APG turbulent boundary layers a second outer peak of the streamwise Reynolds stresses increases with the Reynolds and with pressure gradient to exceed the first inner peak. The inner peak is only weakly affected by the APG as can be seen in figure 3 which includes a comparison of Reynolds stresses of zero pressure gradient TBL at equivalent Reynolds numbers. The position and magnitude of the outer peak of the three turbulence intensity profiles are almost identical for $y^+ > 30$ which indicates a common physics for all velocity components. Lozano-Durán & Bae (2019) have hypothesised that the wall is not the element that organises the momentum-carrying eddies in wall turbulence, whose intensities and sizes are controlled instead by the mean production rate of turbulent kinetic energy with no explicit reference to the distance to the wall. As a consequence, they proposed a characteristic velocity scale based on the shear stress $u^* = \sqrt{-\langle uv \rangle}$ and tested this scaling on channel flows with different mean velocity profiles obtained by different boundary conditions. In the present results of APG TBL the Reynolds stress profiles normalised by the shear stress velocity u^* are constant for wall distances $0.15 < y/\delta < 0.8$ and for all streamwise positions. These constant values 2, 1.3 and 1.8 for the streamwise, wall-normal and spanwise Reynolds stress respectively are the same as for zero pressure gradient TBL of Sillero & Moser (2013) at similar Reynolds numbers (not shown).

In order to understand the physics associated with the growth of the outer peak, the Reynolds Stress tensor budget has been computed along the full simulation domain. The two main components for the turbulent kinetic energy (TKE) budget (production and dissipation) and their sum (the TKE source) are plotted in Fig. 5 for $3000 < Re_\theta < 7000$. As the production is mainly controlled by $\langle uv \rangle \partial U/\partial y$ the outer peak of the production starts to form at $Re_\theta = 4000$ at the same time as the peak of $\langle uv \rangle$ and other Reynolds stresses compo-

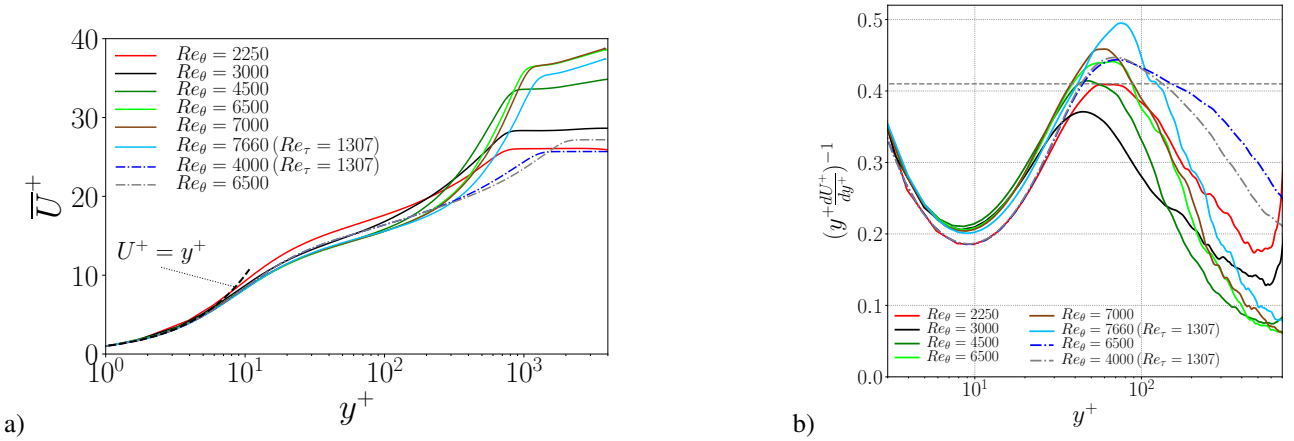

Figure 2. Evolution of the mean velocity profiles at several streamwise positions (a) and the equivalent diagnostic plots to visualise the log region (b). The statistics from ZPG TBL of Sillero & Moser (2013) at similar Reynolds numbers ($Re_\tau = 1307$, $Re_\theta = 4000$) and ($Re_\tau = 2000$, $Re_\theta = 6500$) are plotted for comparison.

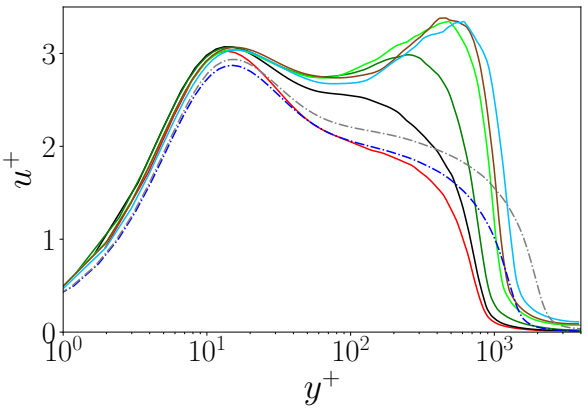

Figure 3. Mean streamwise velocity fluctuation profiles (same legend as figure 2).

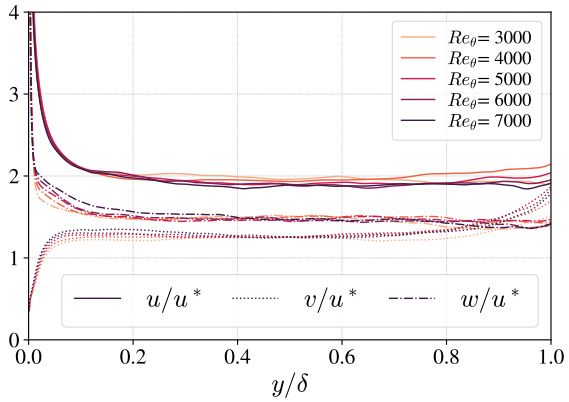

Figure 4. Mean velocity fluctuation profiles normalised by the shear stress velocity $u^* = \sqrt{-\langle uv \rangle}$ at 5 steamwise positions and Reynolds numbers.

nents. The emergence of an outer peak of dissipation is delayed to $Re_\theta > 5000$ which corresponds to 7 local boundary layer thickness downstream. Further downstream, both production and dissipation exhibit an outer peak but the production always exceed the dissipation on a wide range of wall distances from 0.2δ to 0.85δ. The source terms (production + dissipation) which supply the outer peak of kinetic energy corresponds to 20% of the production in this range. Due to a slight vertical shift of the production peak ($y \simeq 0.5\delta$) with respect to the dissipation peak ($y \simeq 0.4\delta$), the maximum source peak stabilises near 0.55δ.

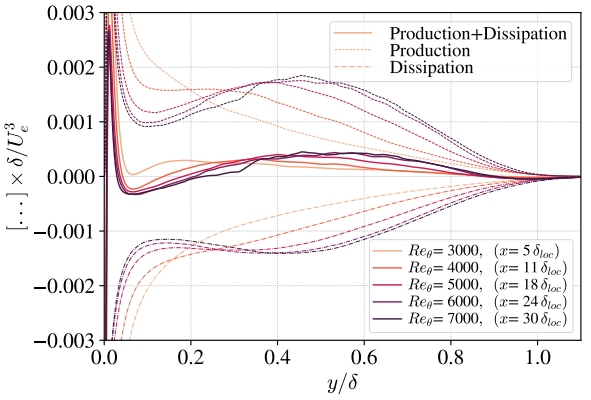

Figure 5. Production and turbulent dissipation rate of turbulent kinetic energy in outer scaling at several streamwise positions.

As can be seen from the Reynolds Stress profiles, the outer peak appears near $y^+ = 100$ at $Re_\theta = 3000$ and moves away from the wall to stabilise before the end of the simulation. For mild APG TBL in equilibrium, the outer peak of turbulence intensity has been located at 1.3 displacement thickness (δ_1) or 0.4 to 0.5 boundary layer thickness (δ) from the wall (see i.e. Kitsios *et al.* (2017)). In the present case of APG out of equilibrium, the peaks of all Reynolds stresses profiles are shown to evolve similarly to reach this wall distance at a streamwise position of the order of 20 local boundary layer thicknesses defined by $x/\delta_{loc} = \int_0^x \delta(x')^{-1} dx'$ (see figure 6b) after the start of the adverse pressure gradient ($x = 0$ in our case). This evolution is in accordance with the experimental results of Cuvier *et al.* (2017) for a similar APG TBL over a long ramp at higher Reynolds numbers ($Re_\theta \simeq 23000$) al-

though the evolution and magnitude of the pressure gradient are not exactly the same. As the two APG flows do not encounter the same history of pressure gradient which extends over a long domain, on which the boundary layer thickness evolves significantly, the choice of local boundary layer thicknesses to normalise the streamwise position seems more pertinent than the averaged one. The extent of the simulation being larger than the experimental one (based on δ_{loc}), the peaks of Reynolds stresses profiles continue to move away for the wall to stabilise near 1.5 displacement thickness or 0.45 boundary layer thickness despite the fact that the pressure gradient starts to decrease at $x/\delta_{loc} = 20$. These results shows that, for a mild pressure gradient, a minimum of 30 local boundary layer thicknesses is needed for the outer peak position to stabilise even when the pressure gradient does not evolve significantly as in the present DNS case. It has been shown that the position of this outer peak is very close to the most external inflection point of the mean velocity profile observed in APG flows (see Shah *et al.* (2010), George *et al.* (2012)). This observation is consistent with the present results. However the mean velocity gradient being almost constant in a wide range of wall distance this inflection point is not well defined and it is not possible to conclude that it coincides with the normal position of the Reynolds stress outer peaks.

Large scale structures

The increase of the outer peak of turbulence intensity at large Reynolds number ZPG TBL is associated with the presence of the very large scale structures of the streamwise fluctuating velocity. These structures are usually decomposed on wall attached structures (self-similar or not) and wall detached ones (see Hwang *et al.* (2020)). The outer peak observed in APG TBL flows is more pronounced and located approximately at the same wall distance. A decomposition of the Reynolds stresses between low and high speed structures shows that for the same volume fraction, the kinetic energy of the high-speed streamwise structures is increased by the effect of APG while the low speed one remains almost unchanged. The two-point correlations of streamwise velocity fluctuations for the current APG TBL have been compared with the DNS results of a ZPG TBL at a lower Reynolds number (see figure 7). The effect of APG is shown to increase the inclination and size of the large scale structures. Moreover, the shape of the correlation function in the buffer layer upstream of the fix point indicates a different organisation in this region with respect to the ZPG TBL. When the fix point is just above the inner peak of u' ($y_o^+ > 50$) associated with near-wall streaks the iso-contours extend much more upstream of the position x_o of fix the point and the near-wall part of the iso-contours linked to the near wall streaks clearly detached from the upper part of the structures (associated with the outer peak of u'). The iso-contours also extend Further downstream and away from the wall to reach 0.8δ. In Figure 8, the two-point correlation function of the streamwise velocity fluctuation conditioned by the sign of $u'(x_o, y_o)$ and normalised by u_τ at the fix point are plotted for different altitudes y_o of the fix point. These results reveal the different behaviours with high-speed large-scale structures (when conditioned by $u'(x_o, y_o) > 0$) which extends more downstream for $y_o < 100^+$ and more upstream for $y_o > 100^+$. As both conditioned correlations are normalised by u_τ the highest iso-contours show that the variance of positive u' is larger than the variance in the negative one for all wall distances y_o. More detailed statistics of each individual structure would be needed to better assess the effect of APG

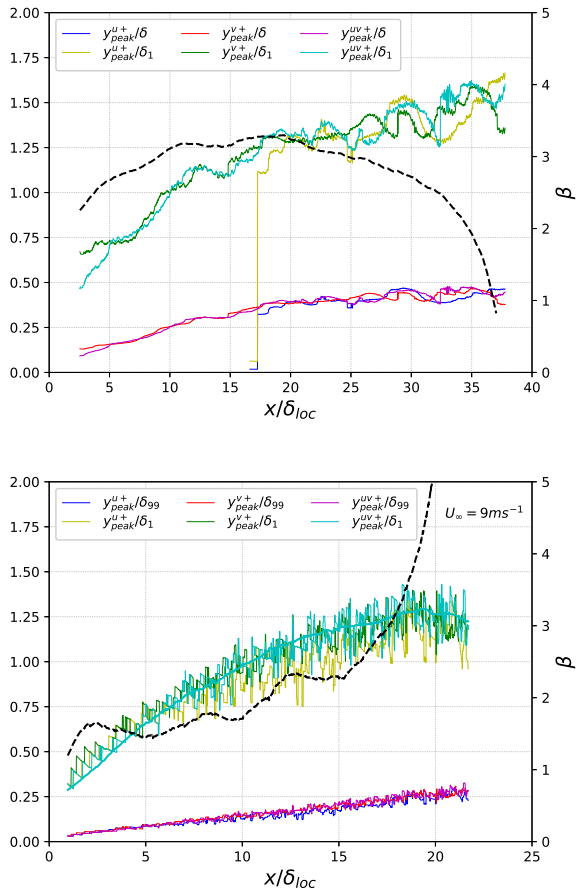

Figure 6. Evolution of outer peak wall normal position of the Reynolds stresses with respect to the boundary layer thickness (δ) and the displacement thickness (δ_1) for (top) the present DNS of APG TBL (bottom) the experimental results of a TBL flow over a ramp at $-5°$ from Cuvier *et al.* (2017) with comparable magnitude although different evolution of adverse pressure gradient $\beta = \frac{\delta_1 U_e}{u_\tau^2}\frac{dU_e}{dx}$ (dash lines, right axis) and higher Reynolds number ($Re_\theta = 23000$). x/δ_{loc} is the position in number of local boundary layer thickness from the start of the APG ($x = 0$).

on these large scale structures. However such statistics would require much more uncorrelated velocity fields than available for the current DNS.

Conclusions

A new DNS of APG TBL over a flat plate has been presented. This simulation is long enough to study the evolution of the Reynolds stress profiles and to follow the growth and stabilisation of the outer peak. This outer peak is located at the same position for all Reynolds stresses and takes more than 25 local boundary layer thicknesses to stabilise near 1.3 boundary layer displacement thicknesses or 0.45δ. The Reynolds stress profiles scale almost perfectly with the shear stress velocity profiles $u^\star$ on a wide range of wall distances from 0.15δ up to 0.8δ, independently of the Reynolds numbers. The APG is shown to have a strong effect on the upstream part of streamwise fluctuating velocity inclined structures as compared to the ZPG case.

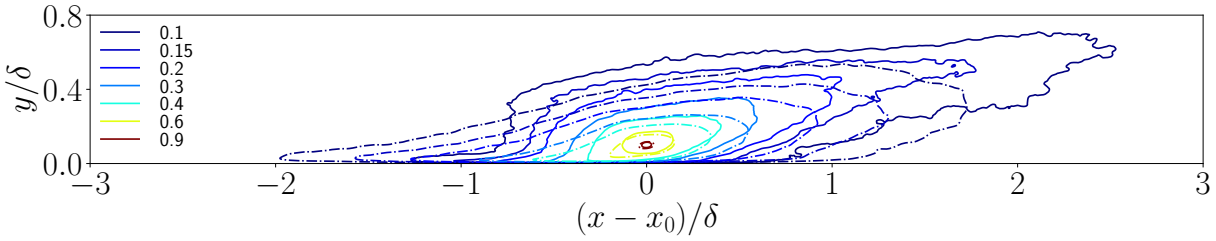

Figure 7. Comparison of the iso-contours of the two-point correlation of the streamwise velocity fluctuation at $y_o = 0.08\delta$ between the present APG case at $Re_\theta = 7240$ (continuous lines) and the ZPG case at $Re_\theta = 2068$ (dash-dotted lines) from Solak & Laval (2018).

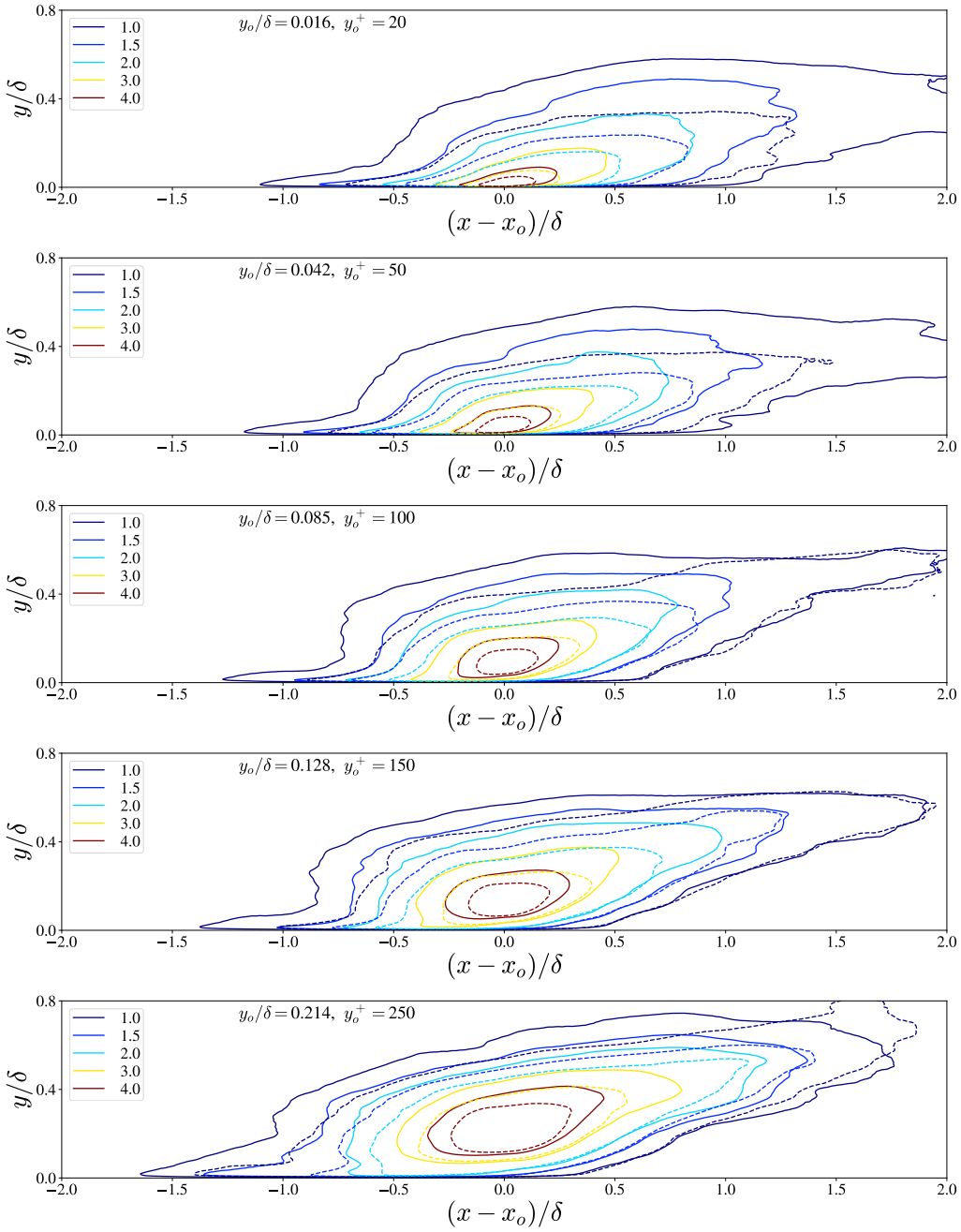

Figure 8. Iso-contours of the two-point correlations of the streamwise velocity fluctuation u' conditioned by $u'(x_o, y_o) > 0$ (continuous lines) and $u'(x_o, y_o) < 0$ (dash lines) for APG case at x_o such that $Re_\theta(x_o) = 7240$. The correlation are normalised by u_τ^2 at the fix point (x_o, y_o)

Acknowledgement

This work was granted access to the HPC resources of IDRIS under the allocation 021741 made by GENCI (Grand Equipment National de Calcul Intensif).

REFERENCES

Cuvier, S., Srinath, S., Stanislas, M., Foucaut, J.-M., Laval, J.-P., Kahler, C. J., Hain, R., Schamowski, S., Schroder, A., Geisler, R., Agocs, J., Rose, A., Willert, C., Klinner, J., Amili, O., Atkinson, C. & Soria, J. 2017 Extensive characterization of a high reynolds number decelerating boundary layer using advanced optical metrology,. *Journal of Turbulence* **18** (10), 929–972.

George, W. K., Stanislas, M. & Laval, J. P. 2012 New insights into adverse pressure gradient boundary layers. In *Progress in Turbulence and Wind Energy IV* (ed. Martin Oberlack, Joachim Peinke, Alessandro Talamelli, Luciano Castillo & Michael Hölling), pp. 201–204. Berlin, Heidelberg: Springer Berlin Heidelberg.

Hwang, J., Lee, J. & Sung, H. 2020 Statistical behaviour of self-similar structures in canonical wall turbulence. *J. Fluid Mech.* **905** (A6).

Kitsios, V., Sekimono, A., Atkinson, C., Sillero, J.A., Borrell, G., Gungor, A.G., Jimenez, J. & Soria, J. 2017 Direct numerical simulation of a self-similar adverse pressure gradient turbulent boundary layer at the verge of separation. *J. Fluid Mech.* **829**, 392–419.

Laizet, S. & Lamballais, E. 2009 High-order compact schemes for incompressible flows: a simple and efficient method with the quasi-spectral accuracy. *J. Comp. Phys.* **228** (15), 5989–6015.

Lee, J. H. 2017 Large-scale motions in turbulent boundary layers subjected to adverse pressure gradients. *J. Fluid Mech.* **810**, 323–361.

Lozano-Durán, A. & Bae, H. J. 2019 Characteristic scales of townsend's wall attached eddies. *J. Fluid Mech.* **868**, 698–725.

Marquillie, M., Ehrenstein, U. & Laval, J.-P. 2011 Instability of streaks in wall turbulence with adverse pressure gradient. *J. Fluid Mech.* **681**, 205–240.

Marquillie, M., Laval, J.-P. & Dolganov, R. 2008 Direct numerical simulation of separated channel flows with a smooth profile. *J. Turbulence* **9** (1), 1–23.

Pozuelo, R., Li, Q., Schlatter, P. & Vinuesa, R. 2022 An adverse-pressure-gradient turbulent boundary layer with nearly constant $\beta \simeq 1.4$ up to $re_\theta \simeq 8700$. *J. Fluid Mech.* **939** (A34).

Schlatter, P., Örl ü, R., Brethouwer, G., Johansson, A. V., Alfredsson, P. H. & Henningson, D. S. 2012 Progress in simulations of turbulent boundary layers .

Shah, S. I., Stanislas, M. & Laval, J.-P. 2010 A specific behavior of adverse pressure gradient near wall flows. In *Progress in wall turbulence : understanding and modelling* (ed. M. Stanislas, J. Jimenez & I. Marusic), pp. 257–265. Villeneuve d'Ascq, France, April 21-23: Springer.

Sillero, J. A. Jiménez, J. & Moser, R. D. 2013 One-point statistics for turbulent wall-bounded flows at Reynolds numbers up to +2000. *Phys. Fluids* **25** (105102), 1–16.

Solak, I. & Laval, J.-P. 2018 Large-scale motions from a direct numerical simulation of a turbulent boundary layer. *Phys. Rev. E* **98**, 033101.